Article

Quantum Monte Carlo and Density Functional Theory Characterization of 2-Cyclopentenone and 3-Cyclopentenone Formation from O(P) + Cyclopentadiene

Jeffrey C. Grossman, William A. Lester,, and Steven G. Louie

J. Am. Chem. Soc., **2000**, 122 (4), 705-711 • DOI: 10.1021/ja983879f

Quantum Monte Carlo and Density Functional Theory Characterization of 2-Cyclopentenone and 3-Cyclopentenone Formation from O(^{3}P) + Cyclopentadiene

Jeffrey C. Grossman,† William A. Lester, Jr.,*,‡ and Steven G. Louie†

Contribution from the Department of Physics, University of California at Berkeley, and Materials Sciences Division, Lawrence Berkeley National Laboratory, Berkeley, California 94720, and Chemical Sciences Division, Lawrence Berkeley National Laboratory, and Department of Chemistry, University of California, Berkeley, California 94720

Received November 9, 1998. Revised Manuscript Received September 13, 1999

Abstract: We investigate reaction paths for the formation of ground-state 2-cyclopentenone and 3-cyclopentenone arising from the electrophilic addition of O(^{3}P) to a double bond of cyclopentadiene. Our calculations show that one possible mechanism for these reactions is the formation initially of a triplet diradical that undergoes intersystem crossing to a diradical singlet followed by passage of the system through the transition state to ground-state products. Equilibrium geometries and total energies are computed for all species using the Hartree−Fock method, the local spin density approximation, four generalized gradient approximations, the G2 model chemistry method, and the quantum Monte Carlo (QMC) approach in both the variational (VMC) and diffusion (DMC) variants. Using DMC as a gauge of accuracy, a comparison of these approaches reveals that the density functional methods show mixed performance, with the gradient-corrected B3PW91 functional giving the best reaction pathway energetics overall for the group. The G2 energetics are in good agreement with DMC for stable species but differ significantly for transition states. A resonance found in precursors to formation of 3-cyclopentenone (3CP) provides a possible explanation for the appearance of 3CP in trace amounts in cyclopentadiene combustion reactors.

1. Introduction

Cyclopentadiene (CPD) combustion is a subject of considerable practical interest because CPD is one of the major intermediates in the high-temperature oxidation of benzene and toluene[1,2] and is a constituent of diesel fuels. The subsequent reactions of cyclopentadiene in flow reactors are many and complex. In these reactor studies there has been a lack of observable stable intermediates with the exception of trace amounts of 3-cyclopentenone[3] (see Figure 1).

Recently, computational studies of the addition of O(^{3}P) to CPD have appeared. A semiempirical approach was used to model the triplet pathway[4] and an extension of the G2 method to characterize the singlet pathway.[5] With the high accuracy required to model reliably oxidation reactions, we have investigated the formation of 3-cyclopentenone from O(^{3}P) reacting with CPD. It is also of interest to understand the formation of the closely related 2-cyclopentenone.

Oxidation of unsaturated hydrocarbons is an area of high interest in combustion chemistry because of its practical importance for fuel consumption. The accepted mechanism for reactions of O(^{3}P) with unsaturated hydrocarbons involves addition to the double or triple bond to give a triplet diradical. Intersystem crossing leads to formation of a singlet diradical followed by formation of singlet products. In this study we focus on the formation of the singlet products 3- and 2-cyclopentenone. Triplet diradical evolution is not followed here owing to higher energy barriers to reaction.

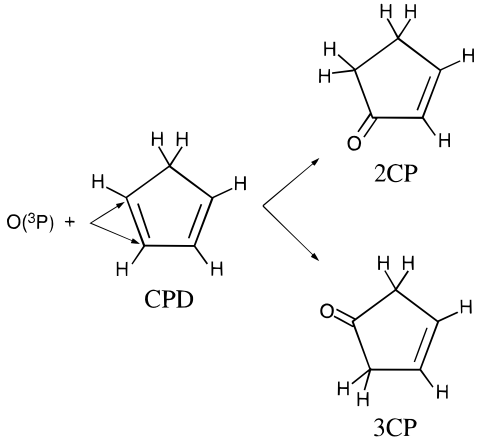

Figure 1. Reactions treated in the present study: O(^{3}P) + cyclopentadiene (CPD) → 2-, 3-cyclopentenone (2CP, 3CP).

We consider the two lowest energy reaction paths corresponding to the two alternative attachment sites of the oxygen atom to the double bond—one site leading to 2-cyclopentenone (2CP) and the other to 3-cyclopentenone (3CP) (see Figure 1). In addition, the energy of a stable epoxide (see Figure 2) has

† Department of Physics, University of California at Berkeley and Materials Sciences Division, Lawrence Berkeley National Laboratory.

‡ Chemical Sciences Division, Lawrence Berkeley National Laboratory and Department of Chemistry, University of California, Berkeley.

(1) Brezinsky, K. *Prog. Energy Combust. Sci.* **1986**, *3*, 1.

(2) Emdee, J. L.; Brezinsky, K.; Glassman, I. *J. Phys. Chem.* **1992**, *96*, 2151.

(3) Glassman, I. 19th Annual Combustion Research Conference Abstract, Department of Energy, Office of Energy Research, Office of Basic Energy Sciences, Chemical Sciences Division, Chantilly, VA, 1997; p 98.

(4) Zhong, X.; Bozzelli, J. W. *Int. J. Chem. Kinet.* **1990**, *29*, 893.

(5) Wang, H.; Brezinsky, K. *J. Phys. Chem. A* **1998**, *102*, 1530.

10.1021/ja983879f CCC: $19.00
Published on Web 01/15/2000

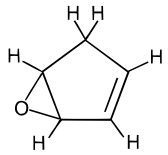

Figure 2. Epoxide molecule formed from O(^{3}P) + CPD; hydrogen atoms are not shown.

been determined. Similar to previous studies of the oxidation of allene[6,7] and ethylene,[8−12] attachment of O(^{3}P) leads initially to triplet diradical states. The open-shell singlet diradical is stable and nearly isoenergetic with the triplet diradical, in accord with the initial step of the O(^{3}P) reaction with ethylene and with allene.

Energy differences must be evaluated with high accuracy if one is to correctly characterize these reactions. In particular, the energy difference between the diradicals (singlet and triplet) and the singlet transition state is extremely challenging to calculate accurately by mean-field methods, e.g., the Hartree−Fock (HF) and the local density approximation (LDA), which typically do not describe well the fine interplay between Coulomb, exchange, and correlation effects for such comparisons. Hydrogen migration, involving the breaking and making of bonds, is also less well described using ab initio basis set expansion and gradient-corrected density functional methods which rely on cancellation of systematic errors of basis sets and density-dependent properties.

The generalized gradient approximations (GGAs) have recently become popular for the prediction of the energetics of chemical reactions and yield significant improvement over the local density approximation. In particular, partial inclusion of the exact Hartree−Fock exchange in the exchange functional[13] has yielded an improved treatment of transition states.[14] However, the trends in improvement are not systematic with GGA methods. For this reason it is useful to assess a computational reaction path characterization obtained with these methods by comparisons with other approaches.

Ab initio basis set expansion methods such as coupled cluster/many body perturbation theory can be used for such purposes in systems of order 1−5 first- and second-row atoms. In these cases, very accurate results may be obtained. Unfortunately, larger systems become increasingly difficult to treat due to the scaling of these methods with number of particles—typically n^7 where n is the number of basis functions.

In the G2 semiempirical method,[15,16] a quadratically convergent configuration interaction (CI) calculation, which ordinarily would be prohibitively demanding, is modeled using a small CI calculation plus corrections based on Moller−Plesset (MP) perturbation theory. This method, which uses a fit to experiment for a large set of molecules formed of first-row atoms, has been shown to be very accurate for a number of molecular properties. However, G2 suffers the same drawback of poor scaling with system size as mentioned above due to the need to do a CI calculation.

Quantum Monte Carlo (QMC), a comparatively recent alternative for high-accuracy calculations, scales more favorably with system size—N^3, where N is the number of electrons of the system. (There is also a dependence on atomic number Z, which with the use of effective core potentials leads to a $\sim Z_{\mathrm{eff}}^{3,4}$ dependence,[17,18] where Z_{eff} is the effective atomic number). Notwithstanding these dependencies, QMC calculations have been carried out on larger systems than have been treated using CCSD(T) (coupled cluster with single, double, and perturbation incorporation of triple excitations), owing to the computational requirements of the latter approach using GAUSSIAN94.[19] In that work it was determined that QMC, in the diffusion Monte Carlo variant, scales similarly to the Hartree−Fock and local density approximations.

In this study we employ eight theoretical approaches, including HF, LDA, GGA, G2, and QMC, to calculate critical points and stable intermediates on the multidimensional potential energy surface, as well as heats of reaction and atomization energies of the stable molecular species. The predictive capability of each of these methods is assessed. The application of a range of state-of-the-art computational techniques enables us to (i) further understand these particular combustion reactions, (ii) make predictions of chemical accuracy, and (iii) assess accuracy among a number of commonly used theoretical approaches. The CCSD(T) approach is not included in these comparisons owing to its computational demands.

2. Computational Methods

In the present QMC approach,[20,21] both variational and diffusion Monte Carlo methods are used to obtain energies of quantum many-body systems. We use variational Monte Carlo (VMC)[22,23] method to construct an optimized correlated many-body trial function $\psi_T(R)$, as a product of Slater determinants D_n and a correlation factor,[24,25]

$$\psi_T = \sum_n \mathrm{d}n\, D_n^{\uparrow} D_n^{\downarrow} [\sum_{i,j} u(r_{iI}, r_{jI}, r_{ij})] \qquad (1)$$

Here, I labels the nuclei, i, j denote electrons, and r_{iI}, r_{jI}, r_{ij} designate interparticle distances. Parametrization and optimization of $u(r_{iI}, r_{jI}, r_{ij})$, which represents the electron−electron, electron−nucleus, and electron−electron−nucleus correlations, is described in ref 26. In the Slater determinant, we employ natural orbitals rather than HF orbitals which have been shown to improve the quality of the QMC trial function.[19,27]

(6) Hammond, B. L.; Huang, S.-Y.; Lester, W. A., Jr.; Dupuis, M. *J. Phys. Chem.* **1990**, *94*, 7969.
(7) Schmoltner, A. M.; Huang, S. Y.; Brudzynski, R. J.; Chu, P. M.; Lee, Y. T. *J. Chem. Phys.* **1993**, *99*, 1644.
(8) Dupuis, M.; Wendoloski, J. J.; Takada, T.; Lester, W. A., Jr. *J. Chem. Phys.* **1982**, *76*, 481.
(9) Dupuis, M.; Wendoloski, J. J.; Lester, W. A., Jr. *J. Chem. Phys.* **1982**, *76*, 488.
(10) Schmoltner, A. M.; Chu, P. M.; Brudznski, R. J.; Lee, Y. T. *J. Chem. Phys.* **1989**, *91*, 6926.
(11) Buss, R. J.; Baseman, R. J.; He, G.; Lee, Y. T. *J. Photochem.* **1981**, *17*, 389.
(12) Lester, W. A., Jr.; Dupuis, M.; O'Donnel, T. J.; Olson, A. J. In *Frontiers of Chemistry*; Laidler, K. J., Ed.; Pergamon: Oxford, 1982; p 159.
(13) Becke, A. D. *J. Chem. Phys.* **1993**, *98*, 5648.
(14) Durant, J. L. *Chem. Phys. Lett.* **1996**, *256*, 595.
(15) Pople, J. A.; Head-Gordon, M.; Fox, D. J.; Raghavachari, K.; Curtiss, L. A. *J. Chem. Phys.* **1989**, *90*, 5622.
(16) Curtiss, L. A.; Raghavachari, K.; Trucks, G. W.; Pople, J. A. *J. Chem. Phys.* **1991**, *94*, 7221.
(17) Ceperley, D. M. *J. Stat. Phys.* **1986**, *43*, 815.
(18) Hammond, B. L.; Reynolds, P. J.; Lester, W. A., Jr. *J. Chem. Phys.* **1987**, *87*, 1130.
(19) Grossman, J.; Mitas, L. *Phys. Rev. Lett.* **1997**, *79*, 4353.
(20) Mitas, L.; Shirley, E. L.; Ceperley, D. M. *J. Chem. Phys.* **1991**, *95*, 3467.
(21) Greeff, C. W.; Lester, W. A., Jr.; Hammond, B. L. In *Recent Advances in Quantum Monte Carlo Methods*; Lester, W. A., Jr., Ed.; World Scientific: Singapore, 1999; p 117.
(22) Hammond, B. L.; Lester, W. A., Jr.; Reynolds, P. J. *Monte Carlo Methods in Ab Initio Quantum Chemistry*; World Scientific: Singapore, 1994.
(23) Ceperley, D. M.; Mitas, L. *Quantum Monte Carlo Methods in Chemistry, Advances in Chemical Physics*; John Wiley: New York, 1996; Vol. XCIII.
(24) Schmidt, K. E.; Moskowitz, J. W. *J. Chem. Phys.* **1990**, *93*, 4172.
(25) Fahy, S.; Wang, X. W.; Louie, S. G. *Phys. Rev. Lett.* **1988**, *61*, 1631.

Single-reference trial functions were used for all of the systems studied. Weights for CI computations of the ground-state configuration state function are found to be 0.96−0.98 for all species considered here, indicating that multireference wave functions are likely to have little impact on our computed results. For a number of cases, we also performed multiconfiguration self-consistent field calculations that included wave function reoptimization, and we again found very weak mixing of higher excitations with the ground state. For the triplet diradical states, we used restricted open-shell wave functions as QMC trial functions and unrestricted wave functions for the LDA and GGA calculations.

Diffusion Monte Carlo (DMC) is based on the property that the operator $\exp(-\tau H)$, where H is the Hamiltonian, projects out the ground state of any trial function with the same symmetry and nonzero overlap, and is used to remove most of the remaining variational bias.[22,23,28] In DMC, one simulates stochastically the imaginary-time Schrödinger equation,

$$f(R,t+\tau) = \int G(R,R';\tau) f(R',t)\, dR' \qquad (2)$$

where $f(R,t) = \psi_T(R)\phi(R,t)$, $G(R,R';\tau)$ is a Green function which is known in the $\tau \rightarrow 0$ limit,[24,29] and $\phi(R,t)$ is the asymptotic solution to the time-dependent Schrödinger equation in imaginary time. Effective core potentials[30] are used to eliminate atomic cores for C and O.

In addition to DMC, we have also calculated reaction path energetics using the LDA,[31,32] four GGAs, and the G2 methods. For LDA, we employ the parametrization of Vosko et al.[33] of the exact uniform gas results of Ceperley and Alder[34] (this corresponds to the SVWN5 method in GAUSSIAN94[35]). For the GGAs, we have used the currently most popular functionals, namely BLYP,[36,37] B3LYP,[13,37] BPW91,[36,38] and B3PW91.[13,38] The HF, LDA, GGA, and G2 calculations were carried out with the GAUSSIAN94 package[35] on SGI Origin2000 machines. The G2 method was implemented as described in ref 16. We were unable to carry out CCSD(T) calculations using basis sets larger than cc-pVDZ[39] with the G94 and G98 packages due to computer time requirements and storage limitations.

Extensive basis sets were employed with each method for all species considered. As shown in our study of C_5H_6,[40] converged energies require the cc-pVQZ basis set which is employed in all present calculations. For geometry optimization, the 6-311G** basis set was used in all cases. Larger basis sets were found to have very little effect on geometries.[40] DMC calculations do not have the strong basis set dependence typical for ab initio post-HF expansion methods, although they require a precise wave function in the vicinity of nuclei. To this end, we computed numerical atomic HF orbitals which formed part of the basis set for the DMC trial wave functions.

Table 1. Selected Optimized Structural Information for Cyclopentadiene (CPD),[a] 2-Cyclopentenone (2CP), 3-Cyclopentenone (3CP), and Epoxide[b]

CPD

	C_1-C_2	C_2-C_3	C_3-C_4	$\angle C_1C_2C_3$	C_1-H	C_2-H
B3PW91	1.498	1.346	1.464	109.0	1.099	1.082
B3LYP	1.505	1.346	1.469	109.1	1.099	1.081
EXP[c]	1.509(3)	1.342(4)	1.469(3)	109.3(3)	−	−

2CP

	C_1-C_5	C_3-C_4	C_2-C_3	C_4-O	C_1-H	C_3-H
B3PW91	1.536	1.478	1.337	1.208	1.096	1.083
B3LYP	1.540	1.482	1.338	1.210	1.095	1.082

3CP

	C_1-C_5	C_4-C_5	C_3-C_4	C_5-O	C_1-H	C_3-H
B3PW91	1.531	1.499	1.334	1.202	1.097	1.084
B3LYP	1.537	1.505	1.334	1.203	1.096	1.083
EXP[c]	1.524(10)	1.509(10)	1.338(5)	1.210(3)	1.086(5)	1.079(5)

Epoxide

	C_1-C_5	C_4-C_5	C_2-C_3	C_5-O	C_1-H	C_5-H
B3PW91	1.518	1.471	1.335	1.424	1.096	1.086
B3LYP	1.524	1.475	1.335	1.431	1.095	1.085

[a] Numbering of the carbons begins with the carbon with the two hydrogens and increases sequentially clockwise. The ordering is retained for the other molecules with orientation shown in Figures 1 and 2. [b] Results are given (in angstroms and degrees) for the B3PW91 and B3LYP methods using the 6-311G* basis and experiment. [c] Reference 45.

3. Structural Properties

All molecular structures reported in this work are fully optimized geometries determined using the given method, with the exception of DMC; in the latter case we used B3LYP-optimized geometries. As expected, the LDA approach gives good geometries. The BPW91 and BLYP methods do not improve, on average, upon LDA structures. However, use of the B3 exchange functional does lead to small improvements.

Structures optimized with the B3LYP and B3PW91 methods are given in Table 1 for CPD, 2CP, 3CP, and the epoxide. For CPD and 3CP, comparison of bond distances and angles with experiment shows that both methods perform well. Overall, B3LYP is in better accord with experiment, in agreement with previous work,[14,41] and so we have used B3LYP geometries for DMC calculations.

It is important to understand the impact on energetics of using B3LYP-optimized geometries for DMC. For each structure we evaluated the effect of using the optimized geometries of different methods on energies computed in the HF, LDA and several GGA approaches. We found, for the species involved in these reactions, rather flat regions of the potential energy surfaces near the optimal geometries. As a result, deviations in total energies with a given method among geometries which were optimized by other methods are minimal. For example, the total energies of the transition state leading to 2-cyclopentenone for the BPW91 and B3LYP geometries differ by 1.4 kcal/mol with HF and 0.6 kcal/mol with LDA. Similar differences are observed for other species. For the subject reactions, energies are found not to be very sensitive to the method used for geometry optimization.

(26) Mitas, L. Pseudopotential quantum Monte Carlo for large-z atom systems. In *Computer Simulation Studies in Condensed-Matter Physics V*; Landau, D., Mon, K., Schuttler, H.-B., Eds.; Springer Proceedings in Physics; Springer-Verlag: Berlin, 1993.
(27) Grossman, J. C.; Mitas, L. *Phys. Rev. Lett.* **1995**, *74*, 1323.
(28) Anderson, J. B. *Int. Rev. Phys. Chem.* **1995**, *14*, 85. Anderson, J.-B. *Rev. Comput. Chem.* **1999**, *13*, 133.
(29) Reynolds, P. J.; Ceperley, D. M.; Alder, B. J.; Lester, W. A., Jr. *J. Chem. Phys.* **1982**, *77*, 5593.
(30) Stevens, W. J.; Basch, H.; Krauss, M. *J. Chem. Phys.* **1984**, *81*, 6026.
(31) Hohenberg, P.; Kohn, W. *Phys. Rev.* **1964**, *136*, B864.
(32) Kohn, W.; Sham, L. J. *Phys. Rev.* **1965**, *140*, A1133.
(33) Vosko, S. H.; Wilk, L.; Nusair, M. *Can. J. Phys.* **1980**, *58*, 1200.
(34) Ceperley, D. M.; Alder, B. J. *Phys. Rev. Lett.* **1980**, *45*, 566.
(35) Frisch, M. J.; Trucks, G. W.; Schlegel, H. B.; Gill, P. M. W.; Johnson, B. G.; Robb, M. A.; Cheeseman, J. R.; Keith, T.; Petersson, G. A.; Montgomery, J. A.; Raghavachari, K.; Al-Laham, M. A.; Zakrzewski, V. G.; Ortiz, J. V.; Foresman, J. B.; Cioslowski, J.; Stefanov, B. B.; Nanayakkara, A.; Challacombe, M.; Peng, C. Y.; Ayala, P. Y.; Chen, W.; Wong, M. W.; Andres, J. L.; Replogle, E. S.; Gomperts, R.; Martin, R. L.; Fox, D. J.; Binkley, J. S.; Defrees, D. J.; Baker, J.; Stewart, J. P.; Head-Gordon, M.; Gonzalez, C.; Pople, J. A. *GAUSSIAN94*, Revision B.1; Gaussian, Inc.: Pittsburgh, PA, 1995.
(36) Becke, A. D. *Phys. Rev. A* **1988**, *38*, 3098.
(37) Lee, C.; Yang, W.; Parr, R. G. *Phys. Rev. B* **1988**, *37*, 785.
(38) Perdew, J. P. In *Electronic Structure of Solids '91*; Ziesche, P., Eschrig, H., Eds.; Akademie Verlag: Berlin, 1991; p 11.
(39) Dunning, T. H., Jr. *J. Chem. Phys.* **1989**, *90*, 1007.
(40) Grossman, J. C.; Lester, W. A., Jr.; Louie, S. G. *Mol. Phys.* **1999**, *96*, 629.
(41) Andzelm, J.; Baker, J.; Scheiner, A.; Wrinn, M. *Int. J. Quantum Chem.* **1995**, *56*, 733.

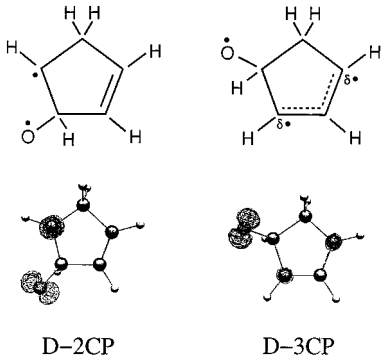

Figure 3. Diradical states labeled D-2CP and D-3CP that lead to products 2CP and 3CP, respectively. Two highest occupied molecular orbitals (calculated within LDA) are shown for each case.

Table 2. Energy Differences (kcal/mol) between the Initially Formed Triplet Diradicals and Reactants[a]

	D-2CP[b]	D-3CP[c]	Δ
HF	−4.0	−8.9	4.9
LDA	−51.6	−66.3	14.7
BPW91	−31.7	−45.5	13.8
BLYP	−29.5	−43.6	14.1
B3PW91	−28.5	−42.1	13.6
B3LYP	−26.8	−40.7	13.9
BGE	−24	−38	14
G2	−21.5	*d*	*d*
DMC	−18(1)	−33(1)	15(2)

[a] The entry Δ denotes the energy difference of the two states. [b] D-2CP, diradical precursor to 2CP. [c] D-3CP, diradical precursor to 3CP. [d] The G2 calculation for D-3CP did not converge. Assuming $\Delta \approx 14$ kcal/mol based on the other methods, we estimate the G2 D-3CP energy to be ∼35.5 kcal/mol.

4. Diradical States

As O(^{3}P) approaches C_5H_6, two stable, triplet diradical states are formed, depending on to which carbon atom of a double bond the oxygen atom attaches. The O attachment site determines the remainder of the reaction path (and therefore the final product). Figure 3 shows these two configurations, labeled D-2CP for the triplet diradical precursor of 2-cyclopentenone, and D-3CP for the triplet diradical precursor of 3-cyclopentenone. In addition to atom positions, the LDA-calculated orbitals of the triplet electrons are shown. In each case, one of these electrons is clearly localized on the O atom. For D-2CP the molecular orbital for the second electron is localized on the other carbon atom of the double bond that was broken. In the case of D-3CP, the second electron is shared among three C atom sites, indicating the formation of a resonance between this electron and the electrons from the double bond in the carbon ring, as illustrated in Figure 3.

Table 2 lists the energies of D-2CP and D-3CP with respect to reactants for the various theoretical approaches. Note that in the HF approximation the two diradicals are barely stable with respect to the reactants. In contrast, LDA significantly overstabilizes these molecules relative to reactants. As is typically the case, the correct answer lies somewhere between the extremes of HF and LDA. Our DMC calculations predict D-2CP to lie 18(2) kcal/mol lower in energy than the reactants and D-3CP to be 33(2) kcal/mol lower (Figure 4). While the GGA methods correct for much of the LDA overestimate, it is not enough based on comparison with DMC results, and, on this basis, the GGA results are still ∼10 kcal/mol too low.

We have also performed Benson group equivalency (BGE) calculations which have been used to estimate heats of reaction

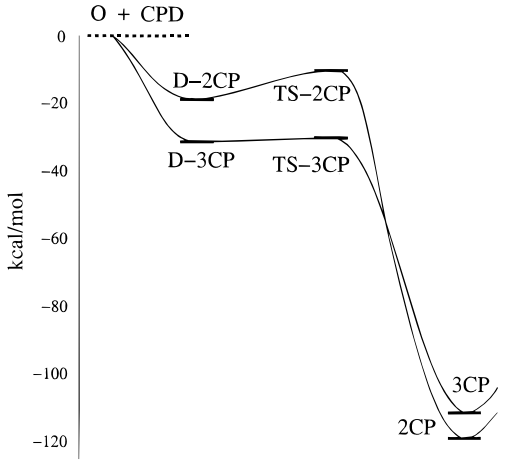

Figure 4. DMC reaction pathways for subject reaction: energy (in kcal/mol) relative to reactants. TS-2CP and TS-3CP denote transition states leading to 2CP and 3CP, respectively.

for organic reactions.[42] Our BGE results for D-2CP and D-3CP (see Table 2) are obtained by consideration of the reactions $C_5H_7OH \rightarrow H_2$ + D-2CP and $C_5H_7OH \rightarrow H_2$ + D-3CP. It is interesting to note that the BGE results place both D-2CP and D-3CP higher in energy than all of the GGA results, in qualitative agreement with the present DMC calculations.

The G2 method is in the best agreement with DMC for the D-2CP energy, with an energy difference of 3 kcal/mol. For D-3CP we were unable to find a minimum-energy structure on the MP2 potential energy surface. We infer a G2 D-3CP energy of 35.5 kcal/mol based on a crude estimate of 14 kcal/mol for the energy difference of the diradical states. This approximation appears reasonable due to the stability of the predicted energy difference between diradical states, as discussed below.

Despite the disagreement among methods for the triplet diradical energies relative to the energy of the reactants, the difference in energy (14−15 kcal/mol) between D-2CP and D-3CP appears remarkably stable across different methods, with the exception of the HF value. For the GGAs, one can perhaps understand this result by considering the homogeneity of electronic charge in each system. With the exception of the region of attachment of oxygen, the diradicals have very similar bonding character and charge distributions, and one may therefore expect a reasonably consistent description of the energy difference since errors are likely to cancel rather well. On the other hand, comparing either D-2CP or D-3CP with O(^{3}P) + C_5H_6, one is considering a greater variety of bonding character and charge densities (i.e., a molecule with one double bond vs an atom plus a molecule with two double bonds). In this case, one may expect less reliable consistency of energy differences due to the fact that the density-dependent errors likely cancel less well.

After O(^{3}P) has attached to form the triplet diradical, an intersystem crossing occurs leading to open-shell singlet molecules. Molecules with electronic structure that violates Hund's rule are currently very difficult to evaluate with GGAs. In contrast, these systems pose no additional difficulties for DMC approaches.[19,20,22] Because of the inability of the GGAs to evaluate the energies of open-shell singlet molecules correctly, we have carried out only DMC calculations for these cases. Geometries are taken from the B3LYP-optimized triplet states. Our results show that the open-shell singlet and triplet diradicals are very close in energy—the difference is within the statistical

(42) Benson, S. W. *Thermochemical Kinetics*; Wiley-Interscience: New York, 1976.

Table 3. Energy Differences (kcal/mol) for the Transition States TS-2CP and TS-3CP Evaluated Relative to the Energy of the Corresponding Diradical State D-2CP and D-3CP

	Δ_{TS}-2CP	Δ_{TS}-3CP
HF	41.6	25.7
LDA	−9.8	−16.2
BPW91	−1.9	−10.4
BLYP	−3.1	−11.8
B3PW91	7.4	−1.7
B3LYP	6.1	−3.2
G2	14.8	−8.7[a]
DMC	8(2)	1(2)

[a] Estimated using $E_{D-3CP} = E_{D-2CP} - 14$ kcal/mol as discussed in footnote *d* of Table 2.

errors of the DMC estimates—in agreement with previous studies of diradical intermediates for smaller molecules.[6,8]

All attempts at searching for a local minimum on the singlet manifold near the diradical geometries resulted in the eventual relaxation through a transition state to a product state. However, transition states were found for both closed-shell singlet pathways. With small structural distortions the molecules can switch from a stable open-shell singlet state to a closed-shell transition state. The minimum energy pathway from these transition states leads to the stable 2CP and 3CP products.

5. Transition States

We performed transition-state searches from a variety of starting points, including both the triplet and open-shell singlet diradical states, as well as several structurally perturbed states. For both paths, i.e., leading to 2CP and 3CP, we found transition states (TS-2CP and TS-3CP) on the closed-shell singlet manifold that lead to the appropriate products.

A close examination of the transition-state geometries reveals that the oxygen atom has moved slightly away from its diradical position. For TS-2CP/TS-3CP the O atom moves in the direction toward/away from the double bond. At the same time, the hydrogen atom begins to migrate away from the oxygen-bonded carbon atom.

Table 3 lists transition-state energy differences, Δ_{TS}, of each method relative to the energy of the corresponding triplet diradical states (i.e., Δ_{TS}-2CP $= E_{TS-2CP} - E_{D-2CP}$ and Δ_{TS}-3CP $= E_{TS-3CP} - E_{D-3CP}$). The HF results for Δ_{TS} are too large and place the transition states much higher in energy than the diradicals. In contrast, LDA gives values for these energy differences that are significantly lower than the DMC results. The LDA underestimate of barriers is typically understood from the increased coordination of transition states relative to reactants combined with the tendency of LDA to overbind, leading to computed barriers that are too low. However, in this case the energy difference is measured from diradical states that are very close in geometry (and therefore coordination) to the transition states. Here the difficulties in predicting accurately Δ_{TS} are entirely due to the *electronic* structure of these molecules. In particular, the tendency of LDA to favor closed-shell molecules over those with higher spin multiplicities is evident in these results, in which the closed-shell transition states are overbound relative to the open-shell, spin triplet diradical states.

Of the GGA approaches, the two hybrid functionals B3LYP and B3PW91 are in closest agreement with DMC values, with differences of only several kilocalories per mole. Our DMC results show that, while the energy difference between the diradical and transition state leading to 2CP is roughly 8 kcal/mol, the transition to 3CP is nearly isoenergetic. With the exception of B3LYP and B3PW91, the other methods do not lead to this finding, and, in fact, the BPW91 and BLYP functionals predict the reverse result, i.e., they favor an isoenergetic transition to 2CP. Present findings support previous studies which have shown that bond-breaking is better described by the hybrid DFT exchange functionals that contain an admixture of part of the exact HF exchange.[43]

The G2 results differ significantly from those of DMC: Δ_{TS}-2CP is about 7 kcal/mol higher and Δ_{TS}-3CP is about 9 kcal/mol lower than the corresponding DMC values. Previous G2 calculations[44] found excellent agreement with experiment for transition-state energies. However, the fact that in the present case the spin multiplicity is different between transition and diradical states may contribute to the present poor agreement between G2 and DMC results.

Table 4. Heats of Reaction (kcal/mol) for Product Systems[a]

	epoxide	2CP	3CP
HF	−33.6	−72.7	−68.3
LDA	−120.0	−148.4	−143.4
BPW91	−88.7	−121.5	−116.2
BLYP	−83.8	−119.9	−114.5
B3PW91	−84.1	−116.7	−111.8
B3LYP	−80.4	−115.9	−110.9
BGE	−83	−120	−114
G2	−86.8	−118.3	−114.2
DMC	−80(2)	−118(2)	−112(2)

[a] $O(^3P) + C_5H_6 \rightarrow$ product.

6. Products

As the reactions proceed from the singlet transition states, the hydrogen atom bonded to the O atom attachment site continues to migrate toward the other carbon of the double bond that was broken. In addition to the product molecules 2CP and 3CP, we have also found a stable epoxide state.

To investigate these products in more detail, a careful examination of the reaction path using internal reaction coordinates has been carried out with the G94 package at the B3LYP/6-311G** level of theory. We take TS-2CP and TS-3CP as initial geometries and step along the reaction path in both the forward and reverse directions. Following the path in the forward direction results in 2CP beginning with TS-2CP and 3CP beginning with TS-3CP. In the reverse direction, both transition states lead to the same epoxide state.

Results for the heats of reaction of these products are given in Table 4. As usual, the HF energies are far too low and the LDA results are too high. The GGAs show mixed performance, with a range of 10 kcal/mol among the different GGA functionals for the heat of reaction to the epoxide. The BLYP and B3PW91 functionals give the best agreement overall with the DMC energies.

Our calculations of BGE heats of reaction for these three species are in very good agreement with the DMC results. We note that the BGE results for the diradicals compare less favorably with DMC than those for the stable product systems, 2CP, 3CP, and the epoxide state. Our G2 results are also in close agreement with the DMC energies.

All methods considered here yield 2CP to be 4−6 kcal/mol lower in energy than 3CP. The existence of 3CP in trace amounts and the absence of 2CP in combustion may have its

(43) Baker, J.; Andzelm, J.; Muir, M.; Taylor, P. R. *Chem. Phys. Lett.* **1995**, *237*, 53.
(44) Durant, J. L.; Rohlfing, C. M. *J. Chem. Phys.* **1993**, *98*, 8031.
(45) *Landolt-Börnstein, New Series II-7*; Hellwege, K.-H., Ed.; Springer-Verlag: New York, 1976.

Table 5. Calculated Atomization Energies (kcal/mol) for the Stable Species with Nine Different Approaches

	CPD	2CP	3CP	epoxide
HF	897.2	969.9	965.6	930.9
LDA	1357.1	1505.5	1500.5	1477.1
BPW91	1188.6	1310.1	1304.8	1277.4
BLYP	1169.6	1289.5	1284.1	1253.5
B3PW91	1186.7	1303.4	1298.4	1270.8
B3LYP	1174.4	1290.0	1285.0	1254.6
G2	1175.4	1293.7	1289.6	1262.2
G2[a]	1179.9	1297.3	1291.9	−
DMC	1181(1)	1300(1)	1294(1)	1261(1)

[a] Modification of G2, ref 5.

origin in the greater stability of the diradical precursor to 3CP relative to 2CP.

7. Atomization Energies

As a further test of the strengths of the various theoretical approaches, we also compare atomization energies for the molecules involved in these reactions (Table 5). Our previous calculation of the CPD atomization energy (AE)[40] demonstrated the need for large basis sets to achieve kilocalorie per mole convergence. Based on that experience, the AEs in Table 5 are computed with the cc-pVQZ basis.

Again the LDA exhibits the usual 20−30% overbinding. The GGA functionals show significant improvement over the LDA, although there is still a range of values depending on the functional used. The B3PW91 functional gives by far AEs in best accord with DMC values.

In Table 5 we have also included atomization energies for CPD, 2CP, and 3CP recently computed by a modified G2 approach.[5] We note that the modified G2 results are several kilocalories per mole closer to the DMC energies than the unmodified G2 calculations. For AEs the G2 method is found to be in closer accord with DMC method than the various GGA approaches.

8. Discussion

This study supports the view that the reactions of $O(^3P)$ + C_5H_6 to form 2-cyclopentenone and 3-cyclopentenone follow the generally accepted mechanism for reactions of ground-state oxygen atom with unsaturated hydrocarbons. This mechanism involves addition to the double or triple bond followed by formation of a triplet diradical. Singlet products arise from the triplet diradical undergoing intersystem crossing to the singlet manifold and singlet diradical followed by passage through a transition state to products. Because of our focus on singlet product molecules, we have not considered the triplet manifold of reaction products. In addition, we have not considered pathways which proceed through the cyclopentadienyl ion nor considered cyclopentadienone, which has been found to be important in high-temperature combustion of benzene and toluene, and pathways leading to noncyclic products.

A notable difference in the pathways is the difference in character of the triplet diradicals, D-2CP and D-3CP. The latter is found to have resonant stability, which may account for 3CP being found in trace amounts in combustors, in contrast to 2CP, which is not found under such conditions. Further consideration of this question lies outside the scope of this study.

The implications of our findings are the following: (i) the electrophilic addition of $O(^3P)$ to CPD may behave similarly to smaller unsaturated hydrocarbon addition reactions (i.e., formation of diradical triplets that lead to singlet transition states and products); (ii) geometries are best described by the B3PW91 and B3LYP methods and are converged with the 6-311G** basis set; (iii) the HF and LDA methods provide a poor description of reaction path energetics, although LDA can give decent geometries; (iv) the GGA functionals BPW91 and BLYP yield better energies than LDA but still possess large errors for some of the energy differences, including Δ_{TS}; (v) the best DFT results are obtained with the hybrid GGA functionals B3PW91 and B3LYP; however, caution must be exercised in their application to reactions owing to nonsystematic errors of the order of 5−10 kcal/mol; (vi) it was not possible to converge the CCSD(T) method; and (vii) good agreement with other high-accuracy approaches (i.e., G2) in the present and previous works combined with favorable scaling suggests that DMC calculations for energetics can be used to characterize accurately reaction paths involving relatively large molecules and complicated processes.

Table 6. Comparison of Computational Time (Hours) and Disk Space (MB) Requirements for One Total Energy Calculation of the Diradical Molecule D-2CP[a]

	cpu	disk	no. of nodes	scaling
LDA	16	<10	8−16	N^3
G2	200	∼20 000	2−4	N^{5-6}
DMC[b]	300	<50	unlimited	N^3

[a] In addition, we list the maximum number of nodes and scaling with number of valence electrons. [B] statistical error of 2 kcal/mol.

At the current level of computational power and algorithm development, no single method can be used to accurately characterize ground-state reactions of the size system considered here with chemical accuracy, i.e., 1−2 kcal/mol. Rather, our experience leads us to suggest that a combination of methods is the best approach. For example, combining the best GGA results for geometries with DMC single-point energy calculations can provide an accurate (∼1−2 kcal/mol) description of the potential energy surface for a given reaction. We suggest such an approach even for larger systems and complicated reaction paths, where it would still be advantageous to perform DMC calculations for some (if not all) of the points on the reaction path in order to check the reliability and accuracy of the GGA functional employed.

It is of interest to compare several important technical details regarding computational demands among the various methods employed here. To this end, we have compared the total CPU time required for a single total energy calculation, the disk space needed to carry out the same calculation, the maximum number of nodes the job can be efficiently run in parallel, and the scaling with number of valence electrons. These comparisons are listed in Table 6 for the calculation of the D-2CP diradical in the LDA, G2, and DMC methods. One notes that LDA calculations are by far the least computationally intensive, and that G2 is roughly 50% faster than DMC (for stochastic error of 2 kcal/mol) for this system. There are substantial differences in scaling with number of electrons among these methods. For disk space, G2 contrasts sharply with DMC and LDA and requires approximately 1000 times more disk storage for this system. The maximum number of nodes is determined by the number of processors for which we were able to perform parallel runs without much loss of efficiency (i.e., almost linear scaling with increasing number of processors). For the LDA and G2 approaches, the maximum number of nodes was determined with the GAUSSIAN94 parallel package. Of course, more efficient parallel algorithms are likely to increase these numbers (we are aware of several LDA calculations which achieve close to linear scaling on up to 64 nodes for small systems). Due to its stochastic nature, the DMC method scales linearly for an

arbitrary number of nodes. This scaling makes DMC an ideal method for massively parallel supercomputer architectures.

9. Conclusions

We have carried out the first comprehensive theoretical study of the oxidation reactions $O(^3P) + C_5H_6 \rightarrow$ 2-, 3-cyclopentenone. The quantum Monte Carlo method in the diffusion Monte Carlo form is found to provide a consistent and accurate description of the reaction pathway. It is shown that one possible mechanism for these reactions is to proceed from initially formed diradical states to corresponding transition states and on to products. The barriers are small, with an essentially barrierless transition in the case of 2CP. In addition, seven other ab initio computational methods are employed in order to compare some of the more commonly used, readily accessible methods for such calculations. We find that HF and LDA have large errors. The GGA methods correct for much of the inaccuracies of LDA; however, nonsystematic trends are found depending on region of the reaction path.

Acknowledgment. The authors acknowledge helpful discussions with Prof. Robert Bergman, Department of Chemistry, University of California, Berkeley. J.C.G. and S.G.L. were supported by National Science Foundation Grant No. DMR-9520554 and by the Director, Office of Science, Office of Basic Energy Sciences, Materials Sciences Division of the U.S. Department of Energy under Contract No. DE-AC03-76SF00098. W.A.L. was supported by the Director, Office of Energy Research, Office of Basic Energy Sciences, Chemical Sciences Division of the U.S. Department of Energy under Contract No. DE-AC03-76SF00098. Computational resources have been provided by NCSA and by NERSC.

JA983879F